https://doi.org/10.26682/sjuod.2022.25.2.2
Journal of University of Duhok., Vol. 25, No.2 (Pure Engineering Sciences), Pp 13-32, 2022

A REVIEW OF STRENGTH AND BEHAVIOR OF REINFORCED CONCRETE BRIDGE DECK SLABS OVERLAID WITH ULTRA HIGH-PERFORMANCE CONCRETE (UHPC)

SIVER IBRAHIM ISMAEL* and GHAFUR H. AHMED**
*Dept. of Civil Engineering, Technical Engineering College, Erbil Polytechnic University, Kurdistan Region-Iraq
**Dept. of Highway Engineering, Technical Engineering College, Erbil Polytechnic University, Kurdistan Region-Iraq

(Received: February 22, 2022; Accepted for Publication: July 19, 2022)

ABSTRACT

The use of Ultra High-Performance Concrete (UHPC) for repairing damaged structures has been discovered in recent decades. Unique properties of UHPC give superior structural performance for strengthening the existing bridge or slab. The lack of data has been available in code provisions about this strengthening technology, that is why reviewing the experimental studies can guide application. This literature study presented the experimental database with its evaluation for the number of researchers to examine the effectiveness of strengthening bridges or slabs with UHPC. Also, this study discussed the basic parameters which affect the strengthening process directly, including interface preparation, size effect, characteristics of substrate NSC and characteristics of UHPC overlay. Different failure modes of composite structures were identified under flexure. In addition, based on the existing works of literature an estimate equation has been developed to predict the cracking and failure load of strengthening composite structures. The experimental studies evidenced that the UHPC can prolong the life of existing old structures and reduce the cost of maintenance. Finally, some recommendations are suggested for future work to obtain a more accurate result.

KEYWORDS: UHPC, Bridge, Composite Slab, Overlay, Failure, and Concrete Interface.

INTRODUCTION

The Bridge deck slab is one of the basic loads carrying components of a rectangular layout which is supported directly on the substructures or perpendicular to the support component (AASHTO, 2017) C5.12.2.1. The Deck slab is used as a base for the roadway, railway, pedestrian walkway, and many other facilities, that is why the bridge deck is resistant to cracks and heavy loads continuously. Therefore, the subject of bridge maintenance and development requires significant research and should be considered seriously. So, when designing a bridge, it is very important to give significant attention to decks to obtain good serviceability, safety, appearance, and many other properties because the deck slabs have an important role in providing the aesthetic appearance of the bridge. Furthermore, structurally it has the advantage of reducing deflection and resisting to the moment greatly (Gunavathy & Indumathi, 2011).

Overlaying the bridge deck slab with a suitable material is one of the successful methods for bridge maintenance and service that prolong the life of bridge and behave like a covering coat for the structure. All around the world, several materials were experimentally investigated to be used as an overlay material for bridge deck slabs but were structurally deficient before reaching their design service life. Selecting a suitable material for the overlay requires wide investigation because bridges are subject to high live load due to traffic volume. Usually, bridges are overlaid with some materials such as (NSC, Bituminous, Latex modified concrete, Silica fume modified concrete, Low slump dense concrete, etc.) which cause failure due to weak resistance to tension force and many other deficiencies. Usually, the most common bridge deck deterioration occurs at cracking places that cause water to penetrate or ion down then causing corrosion of steel rebars. Further damage occurs due to freeze-thaw cycles and wheel dynamic loads. A thin layer of UHPC solved all deficiencies that

siver.mce20@epu.edu.iq

existed previously (Wibowo & Sritharan, 2018). Furthermore, decks have to be overlaid with a suitable material to obtain a wearing surface and protect water or ions ingress which in result may lead to corrosion of steel.

With the advance in knowledge, UHPC has developed and replaced all of the deficiencies that were present in other types of concrete. This new generation of concrete gives the ability to construct structural members with a longer span, lighter in weight, and larger in size (Bajaber & Hakeem, 2021; Wu, Li, & Su, 2018). Also, it is used for overlay application widely due to its superior properties which consist of very low permeability, good freeze-thaw resistance, good bond to concrete, and many others (Aïtcin, 2016; Bajaber & Hakeem, 2021; Du et al., 2021; Haber, Munoz, & Graybeal, 2017). These super properties of this kind of concrete belong to the essential ingredients that consist of steel fiber and silica fumes that impose the ductility in compression and influence cracking behavior through control extending of crack (Aldred et al., 2006; Larsen & Thorstensen, 2020). In addition, failure in the UHPC overlay will happen rarely because the unique strength of UHPC doesn’t permit penetration of cracks into it (Muñoz & Ángel, 2012; Zhu et al., 2022).

In different countries, numerous experimental studies were conducted about bridge or slab maintenance and repair with UHPC with different characteristics and methods but the existential problem of international code for this subject made the reviewing of existing literature become a significant study to guide the practical application.

This study established the experimental databases to examine the effect of strengthening characteristics and discussed in detail the influence of each one which consists of overlay material compressive strength, thickness, reinforcement ratio, with substrate size dimension, compressive strength, reinforcement ratio and surface preparation. Also, depending on the discussed numerical databases the prediction equation is developed that guide the investigators to predict the crack pattern, ultimate load capacity and the region of failure. The most common three regions of failure are Failure at the bond line, Failure in a substrate, and Failure in an overlay (Hussein, Walsh, Sargand, & Steinberg, 2016). For a bridge deck slab overlay with UHPC, proper substrate surface preparation has to be taken into consideration. Most cases of failure occur in the concrete substrate if adequate bond strength is served by good surface preparation.

1 EXPERIMENTAL DATABASES

Nowadays UHPC is the most successful material proposed for overlay Bridge deck slabs compared with other types of overlay materials like conventional concrete, Latex Modified Concrete, Asphalt Concrete Pavement, Micro silica Concrete, and many others. UHPC is accurately designed for many purposes in building construction significantly for overlay bridge deck slabs. UHPC properties of sufficient bond with substrate material and ability to resist cracking due to existing discontinuous steel fibers made it a desirable material for bridge deck slabs overlay. The unique dense matrix of UHPC resists the penetration of chloride ions to the base material which is associated with the corrosion of substrate steel bars. Many studies experimentally evaluated bridges or slabs overlay as summarized in table 1. In this table one-hundred, five slabs and bridges are examined in twenty-five references. This table consists of a description of the properties of two basic parts substrate and overlay, depending on the influence of basic parameters. Substrate parameters consist of the effect of dimension, substrate material compressive strength, reinforcement ratio, and surface preparation. Also, for the application of overlay, the following parameters are taken into consideration material type, compressive strength, thickness, and reinforcement ratio. The databases in table 1 were used to determine the damage degree of the strengthening procedure. In each experimental study, the region of failure was reviewed which includes three basic regions; bond, substrate, and overlay. In addition, according to the types of the experiment the failures are listed which consist of ultimate load, ultimate moment, maximum bond strength, tensile strength, and punching strength.

1.1 Failure regions

Three essential types of failure identified in the experimental database consist of substrate failure (SF), interface failure (IF), and overlay failure (OF). The types of failure are closely related to the substrate and overlay material characterization with interface preparation. Table 1 presented that mainly failure occurs at the substrate or interface. However, adequate bond strength is served by a proper surface preparation but there exist various parameters that have affected the mode of failure which are discussed below in detail. Also, table 1 presented that overlay failure will happen rarely with UHPC material because the unique strength of UHPC doesn’t permit penetration of cracks into it. Only in studies (Ben Graybeal & Haber, 2018; Mohsen A. Issa, Alhassan, & Shabila, 2007), was overlay failure observed in which latex modified concrete and micro-silica concrete was used for the application of overlay. In (Hussein et al., 2016; Muñoz & Ángel, 2012; Sadek et al., 2019; Sritharan & Aaleti, 2017; Tayeh, Abu Bakar, & Megat Johari, 2012; Yang Zhang, Zhang, Zhu, Cao, & Shao, 2020; Yang Zhang, Zhu, Wang, & Wu, 2020)observed failure happened partially at the substrate and partially propagated through the interface, this type is also considered as interface failure.

Table 1: the experimental database of UHPC as overlay material.

Ref.	No.	Substrate							Overlay				Failure Region	Result
		L (mm)	**Cross Section**		**Substrate Material& Strength (MPa)**	**Rf. Ratio %**	**fy (MPa)**	**Surface Preparation (mm)**	**Overlay Material& Strength (MPa)**	**Thick ness (mm)**	**fy (MPa)**	**Rf. Ratio %**		
			b (mm)	**H (mm)**										
(Luo, 2002)	1	127	127	38	NSC fc'42	0	0	R.+L.B.Sy& Et H2O	LMC fc'47	38	0	0	SF	17.92 kN Maximum failure load
	2	127	127	38	NSC fc'42	0	0	R.+L.B.Sy& Et H2O	MMC fc'57	38	0	0	SF	10.18 kN Maximum failure load & 1.82 MPa Maximum shear strength
	3	127	127	38	NSC fc'42	0	0	R.+L.B.Sy& Et H2O	MMC-FA fc'49	38	0	0	SF	13.23 kN Maximum failure load & 2.41 MPa Maximum shear strength
	4	127	127	38	NSC fc'42	0	0	R.+L.B.Sy& Et H2O	FR.C fc'61	38	0	0	SF	11.54 kN Maximum failure load & 2.1 MPa Maximum shear strength
(Habel, 2004)	5	-	1000	152	NSC fc'40	0.9	500	1/2R.C.Z.	UHPC fc'150	50	500	2	SF	Strengthening Detail alone
(Buitelaar, Braam, & Kaptijn, 2004)	6	-	-	-	S.B.Deck	0	-	Exy+Silica Agg.	HPC fc'117	50	0	0	IF	2.96 MPa Bond strength
	7	-	-	-	S.B.Deck	0	-	Exy+Hyperit Agg.	HPC fc'117	50	0	0	IF	4.81 MPa Bond strength
	8	-	-	-	S.B.Deck	0	-	Weld Mesh Rf	HPC fc'117	50	-	-	U.L.P.Stress	-
(Mohsen A. Issa et al., 2007)	9	8500	1800	200	Precast C.	-	-	Exy	LMC fc'47	25	0	0	OF	-
	10	8500	1800	200	Precast C.	-	-	Exy	MSC fc'51	25	0	0	OF	-
	11	8500	1800	200	Precast C.	-	-	S.B.	LMC fc'47	25	0	0	SF	2.1 MPa Bond strength
	12	8500	1800	200	Precast C.	-	-	S.B.	MSC fc'51	25	0	0	SF	2.3 MPa Bond strength
(Perez, Bissonnette, Gagné, &	13	3000	1000	200	NSC fc'45	-	-	Scarification	CFC fc'55	80	-	-	SF	2.60 MPa Direct shear strength
	14	3000	1000	200	NSC fc'45	-	-	S.B.	CFC fc'55	80	-	-	SF	2.42 MPa Direct shear strength

siver.mce20@epu.edu.iq

structures, 2009)	15	3000	1000	200	NSC fc'45	-	-	J.H.+S.B.	CFC fc'55	80	-	-	IF	1.81 MPa Direct shear strength
	16	3000	1000	200	NSC fc'45	-	-	H.P.W.J.	CFC fc'55	80	-	-	SF	2.71 MPa Direct shear strength
(Shann, 2012)	17	3000	1000	150	NSC fc'30	-	-	A-F.B.	UHPC fc'117	25	0	0	Clarified in 2.4.1&2.5.2	0.09 MPa Debonding stress & 0.48 MPa Interface shear stress
	18	3000	1000	250	NSC fc'30	-	-	A-F.B.	UHPC fc'117	25	0	0	Clarified in 2.4.1&2.5.2	0.04 MPa Debonding stress & 0.17 MPa Interface shear stress
	19	3000	1000	200	NSC fc'30	-	-	A-F.B.	UHPC fc'117	6.3	0	0	Clarified in 2.4.1&2.5.2	0.03 MPa Debonding stress & 0.16 MPa Interface shear stress
	20	3000	1000	200	NSC fc'30	-	-	A-F.B.	UHPC fc'117	12.7	0	0	Clarified in 2.4.1&2.5.2	0.05 MPa Debonding stress & 0.25 MPa Interface shear stress
	21	3000	1000	200	NSC fc'30	-	-	A-F.B.	UHPC fc'117	19	0	0	Clarified in 2.4.1&2.5.2	0.055 MPa Debonding stress & 0.33 MPa Interface shear stress
	22	3000	1000	200	NSC fc'30	-	-	A-F.B.	UHPC fc'117	25	0	0	Clarified in 2.4.1&2.5.2	0.06 MPa Debonding stress & 0.37 MPa Interface shear stress
	23	3000	1000	200	NSC fc'30	-	-	A-F.B.	UHPC fc'117	50	0	0	Clarified in 2.4.1&2.5.2	0.08 MPa Debonding stress & 0.48 MPa Interface shear stress
(Tayeh et al., 2012)	24	100	100	150	NSC fc'38	0	0	N.R.	UHPC fc'170	150	0	0	SF+IF	169 kN Max. force & 8.5 MPa Shear stress
	25	100	100	150	NSC fc'38	0	0	S.B.	UHPC fc'170	150	0	0	SF	343 kN Max. force & 17.17 MPa Shear stress
	26	100	100	150	NSC fc'38	0	0	W.B.	UHPC fc'170	150	0	0	SF+IF	232 kN Max. force & 11.65 MPa Shear stress
	27	100	100	150	NSC fc'38	0	0	D.H.	UHPC fc'170	150	0	0	SF+IF	221 kN Max. force & 11.1 MPa Shear stress
	28	100	100	150	NSC fc'38	0	0	G.H.	UHPC fc'170	150	0	0	SF+IF	277 kN Max. force & 13.89 MPa Shear stress
(Muñoz & Ángel, 2012)	29	393.7	100	38.1	NSC fc'31	0	0	Sm-0.6	UHPC-Ductal	38.1	0	0	SF+IF	3.84 MPa Indirect tensile strength
	30	393.7	100	38.1	NSC fc'31	0	0	Chp.-0.92	UHPC-Ductal	38.1	0	0	SF	4.28 MPa Indirect tensile strength
	31	393.7	100	38.1	NSC fc'31	0	0	Br.-0.7	UHPC-Ductal	38.1	0	0	SF+IF	3.33 MPa Indirect tensile strength
	32	393.7	100	38.1	NSC fc'31	0	0	S.B.-1.06	UHPC-Ductal	38.1	0	0	SF+IF	3.77 MPa Indirect tensile strength

	33	393.7	100	38.1	NSC fc'31	0	0	G.	UHPC-Ductal	38.1	0	0	SF+IF	5.72 MPa Indirect tensile strength
(Hussein et al., 2016)	34	-	75	75	NSC fc'41	0	0	Sm.	UHPC fc'158.5	75	0	0	SF+IF	13.22 kN Max. force & 3.02 MPa Shear stress
	35	-	75	75	NSC fc'41	0	0	S.B.	UHPC fc'158.5	75	0	0	SF+IF	21.48 kN Max. force & 5.01 MPa Shear stress
	36	-	75	75	NSC fc'41	0	0	R.	UHPC fc'158.5	75	0	0	SF	24.24 kN Max. force & 5.63 MPa Shear stress
(Bao, Valipour, Meng, Khayat, & Chen, 2017)	37	450	200	25	NSC fc'50	-	-	Calcium hydroxide	UHPC fc'124	25	0	0	IF	1.31 MPa Bond strength
(Sritharan & Aaleti, 2017)	38	2400	609.6	203.2	NSC fc'31.3	0.627	-	Sm	UHPC fc'106.8	30	0	0	SF+IF	311.3 kN Ultimate load & 71.17 (kN.m)/m Ultimate moment
	39	2400	609.6	203.2	NSC fc'31.3	0.627	-	I.G.-1.26	UHPC fc'106.8	30	0	0	SF	311.3 kN Ultimate load & 71.17 (kN.m)/m Ultimate moment
	40	2400	609.6	203.2	NSC fc'31.3	0.627	-	I.G.-3	UHPC fc'106.8	30	0	0	SF	311.3 kN Ultimate load & 71.17 (kN.m)/m Ultimate moment
	41	2400	609.6	203.2	NSC fc'31.3	0.627	-	I.G.-5	UHPC fc'106.8	30	0	0	SF	311.3 kN Ultimate load & 71.17 (kN.m)/m Ultimate moment
(Wibowo & Sritharan, 2018)	42	2400	2400	203.2	NSC fc'45	0.625	517	H.G.	UHPC fc'117	38	517	-	SF	273.92 kN Ultimate load & 124.5 (kN.m)/m Ultimate moment
(Sritharan, Doiron, Bierwagen, Keierleber, & Abu-Hawash, 2018)	43	-	9000	-	Old B.D.	-	-	R.+G. with B.Lth.	UHPC fc'124	38	-	-	SF	1.51 MPa Bond Strength
(Newtson & Weldon, 2018)	44	900	900	101.6	NSC fc'36	0.616	420	R.-2	UHPC fc'123	25.4	0	0	Control Specimen	39.9 kN Ultimate Load
	45	900	900	101.6	NSC fc'36	1.102	420	R.-2	UHPC fc'123	25.4	0	0	Low Shrinkage	39.9 kN Ultimate Load

	46	900	900	152.4	NSC fc'36	0.66	420	R.-2	UHPC fc'123	25.4	0	0	Great Shrinkage	-
	47	300	150	150	NSC fc'36	0	0	L.G.-0.05	UHPC fc'118.8	47.6	0	0	-	7.1 MPa Shear Stress
	48	300	150	150	NSC fc'36	0	0	H.G.-0.9	UHPC fc'118.8	47.6	0	0	-	12 MPa Shear Stress
	49	300	150	150	NSC fc'36	0	0	C.H.-1.6	UHPC fc'118.8	47.6	0	0	-	12 MPa Shear Stress
	50	300	150	150	NSC fc'36	0	0	D.G.-1.6	UHPC fc'118.8	47.6	0	0	-	11.4 MPa Shear Stress
	51	300	150	150	NSC fc'36	0	0	V.G.-1.6	UHPC fc'118.8	47.6	0	0	-	9.8 MPa Shear Stress
	52	300	150	150	NSC fc'36	0	0	R.-2.8	UHPC fc'118.8	47.6	0	0	-	19.8 MPa Shear Stress
(Lapi, Fernandes, Orlando, Ramos, & Lúcio, 2018)	53	2300	2300	150	NSC fc'32	1.84	-	R.	RC.O fc'36	60	-	1.3	IF	580 kN Punching strength
	54	2300	2300	150	NSC fc'34	1.84	-	R.+C.G.	RC.O fc'37	60	-	1.3	IF	590 kN Punching strength
	55	2300	2300	150	NSC fc'26	1.84	-	R.+Dw.	RC.O fc'34	60	-	1.3	P.F.C.S.	568 kN Punching strength
	56	2300	2300	150	NSC fc'25	1.84	-	R.+C.G.+Dw.	RC.O fc'39	60	-	1.3	P.F.C.S.	550 kN Punching strength
(Ben Graybeal & Haber, 2018)	57	30500	8530	430	NSC	-	-	Scarification	LMC-fy3.8	38	-	-	IF	1.8 MPa Peak Tensile Stress
	58	30500	8530	430	NSC	-	-	Scarification	UHPC-fy5.7	38	-	-	IF	0.8 MPa Peak Tensile Stress
	59	30500	8530	430	NSC	-	-	Hydrodemolition	LMC-fy3.8	38	-	-	IF	3 MPa Peak Tensile Stress
	60	30500	8530	430	NSC	-	-	Hydrodemolition	UHPC-fy5.7	38	-	-	SF	3.4 MPa Peak Tensile Stress
	61	30500	8530	430	UHPC Fy5.7	-	-	Scarification	LMC-fy3.8	38	-	-	OF	3.4 MPa Peak Tensile Stress
	62	30500	8530	430	UHPC Fy5.7	-	-	Scarification	UHPC-fy5.7	38	-	-	IF	3.4 MPa Peak Tensile Stress
	63	30500	8530	430	UHPC Fy5.7	-	-	Hydrodemolition	LMC-fy3.8	38	-	-	OF	3.2 MPa Peak Tensile Stress

	64	30500	8530	430	UHPC Fy5.7	-	-	Hydrodemolition	UHPC-fy5.7	38	-	-	IF	4.5 MPa Peak Tensile Stress
(Sadek et al., 2019)	65	2740	810	203	NSC fc'32	-	-	B.F.-2	UHPC fc'107	-	0	0	SF+IF	320 kN Ultimate load
	66	2740	810	203	NSC fc'32	-	-	R.-3	UHPC fc'107	-	0	0	SF	320 kN Ultimate load
	67	2740	810	203	NSC fc'32	-	-	R.-6	UHPC fc'107	-	0	0	SF	347 kN Ultimate load
(Yang Zhang et al., 2019)	68	3200	2000	280	NSC fc'60.2	0.729	400	R.+P.I.S.	UHPC fc'140	50	400	4.16	SF	1295 kN Ultimate load & 970 (kN.m)/m Ultimate moment
(López-Carreño, Carrascón, Aguado, & Pujadas, 2020)	69	2600	1800	310	A.C.P	0	0	S.Anchor	C.C.+P.F fc'50	100	0	0	E.Sh.	4 kN Pull-off test result
	70	2600	1800	310	A.C.P	0	0	R.by Rep.	C.C.+P.F fc'50	100	0	0	Produce Cck.	2.5 kN Pull-off test result
	71	2600	1800	310	A.C.P	0	0	R.by Rep.+Bent Rb.	C.C.+P.F fc'50	100	0	0	H.S.P.	4.5 kN Pull-off test result
(Yang Zhang, Zhu, et al., 2020)	72	300	300	410	NSC fc'30	0.65	453	L.R.-1.78	UHPC fc'128.2	50	453	3.6	IF	472 kN Ultimate load
	73	300	300	410	NSC fc'50	0.65	453	L.R.-2.12	UHPC fc'128.2	50	453	3.6	SF+IF	808.75 kN Ultimate load
	74	300	300	410	NSC fc'50	0.65	453	H.R.-4.56	UHPC fc'128.2	50	453	3.6	SF	1040 kN Ultimate load
	75	300	300	410	NSC fc'50	0.65	453	Ep.Rb-4.14	UHPC fc'128.2	50	453	3.6	SF	1153 kN Ultimate load
	76	300	300	410	NSC fc'50	0.65	453	G.J.	UHPC fc'128.2	50	453	3.6	SF	877.5 kN Ultimate load
	77	300	300	410	NSC fc'50	0.65	453	D.H.	UHPC fc'128.2	50	453	3.6	IF	777.5 kN Ultimate load
	78	300	300	410	NSC fc'50	0.65	453	P.I.S.	UHPC fc'128.2	50	453	3.6	SF	1218.5 kN Ultimate load
(Savino, Lanzoni, Tarantino, & Viviani,	79	1140	820	200	NSC fc'59	-	-	H.R.	UHPFR.C fc'147	50	-	-	SF	Fx vs. slip/debonding 20kN vs. 0.025mm
	80	1140	820	200	NSC fc'59	-	-	H.R.	HPFR.C fc'78	50	-	-	IF	Fx vs. slip/debonding 36kN vs. 0.025mm

2020)														
(Zhu, Zhang, Hussein, Liu, & Chen, 2020)	81	600	600	280	NSC fc'60	0.205	-	R.-(1-4)	UHPC fc'140	50	-	4.18	SF	8.4 MPa Maximum shear stress
(Freeseman, Wang, & Tan, 2020)	82	300	300	80	-	-	-	R.	Exy	9.5	0	0	IF	-
	83	300	300	45	-	-	-	R.	LSDC	40	0	0	IF	-
(Yang Zhang, Zhang, et al., 2020)	84	200	200	250	NSC fc'30	0.523	-	R.-2	UHPC fc'135.5	50	-	2.51	SF+IF	237.7 kN Ultimate load
	85	200	200	250	NSC fc'40	0.523	-	R.-2	UHPC fc'135.5	50	-	2.51	SF+IF	277.3 kN Ultimate load
	86	200	200	250	NSC fc'50	0.523	-	R.-2	UHPC fc'135.5	50	-	2.51	SF	351 kN Ultimate load
	87	200	200	250	NSC fc'50	0.523	-	D.H.-30dp&0.12dm	UHPC fc'135.5	50	-	2.51	SF+IF	356 kN Ultimate load
	88	200	200	250	NSC fc'50	0.523	-	G.J.-10w&10dp	UHPC fc'135.5	50	-	2.51	SF+IF	338.67 kN Ultimate load
	89	200	200	250	NSC fc'50	0.523	-	P.I.S.	UHPC fc'135.5	50	-	2.51	SF+IF	341.67 kN Ultimate load
	90	200	200	250	NSC fc'50	0.523	-	Sm	UHPC fc'135.5	50	-	2.51	SF+IF	216 kN Ultimate load
(Teng, Valipour, & Khayat, 2021)	91	2000	1000	150	NSC fc'37	-	-	R.	CC fc'37	38	0	0	IF	1.5 MPa bond strength
	92	2000	1000	150	NSC fc'37	-	-	R.	CC fc'37	50	0	0	IF	1.2 MPa bond strength
	93	2000	1000	150	NSC fc'37	-	-	R.	LMC fc'46	25	0	0	IF	2.1 MPa bond strength
	94	2000	1000	150	NSC fc'37	-	-	R.	LMC fc'46	38	0	0	IF	1.7 MPa bond strength
	95	2000	1000	150	NSC fc'37	-	-	R.	LMC fc'46	50	0	0	IF	1.5 MPa bond strength

96	2000	1000	150	NSC fc'37	-	-	R.	G50 fc'111	38	0	0	SF	1.9 MPa bond strength
97	2000	1000	150	NSC fc'37	-	-	R.	LWS35 fc'134	38	0	0	SF	2.1 MPa bond strength
98	2000	1000	150	NSC fc'37	-	-	R.	EA5LWS35 fc'120	25	0	0	SF	2.5 MPa bond strength
99	2000	1000	150	NSC fc'37	-	-	R.	EA5LWS36 fc'120	38	0	0	SF	2.7 MPa bond strength
100	2000	1000	150	NSC fc'37	-	-	R.	EA10LWS35 fc'105	25	0	0	SF	2.3 MPa bond strength
101	2000	1000	150	NSC fc'37	-	-	R.	EA10LWS36 fc'105	38	0	0	SF	2.4 MPa bond strength
102	2000	1000	150	NSC fc'37	-	-	R.	EA10LWS37fc'105	50	0	0	SF	2.7 MPa bond strength
103	2000	1000	150	NSC fc'37	-	-	R.	EA10LWS35–3.25 fc'120	25	0	0	SF	2.5 MPa bond strength
104	2000	1000	150	NSC fc'37	-	-	R.	EA10LWS35–3.26 fc'120	38	0	0	SF	2.6 MPa bond strength
105	2000	1000	150	NSC fc'37	-	-	R.	EA10LWS35–3.27 fc'120	50	0	0	SF.	2.2 MPa bond strength

Note: Sm-smooth; I.G.-Inclined Groove; H.G.-Horizontal Groove; D.G.-Diagonal Groove; V.G.-Vertical Groove; R.-Rough; L.R.-Low Roughness; H.R.-High Roughness; B.F.-Broom Finish; G.J.-Grooved Joint; D.H.-Drilled Holes; P.I.S.-Post Installed Steel Stud; Ep. Rb-Exposed Rebars; U.TD-Ultra-High-Performance Tendon; C.H.-Calcium Hydroxide; EA-CaO-based expansive agent; L.B.Sy& Et H2O- Latex Based Slurry & Extra Water; 1/2R.C.Z.-1/2 Roughness of Contact Zone; A-F.B.- Assume Full Bond; L.G.-Lightly Ground; C.H.-Cross Hatch; Chp.-Chipped; Br.-Brush; S.B.-Sandblast; Exy+Silica Agg.-Epoxy with Silica Aggregate; RC.O- Bonded Reinforced Concrete Overlay; C.G.-Cement Grout; Dw.- Dowel; J.H.-Jackhammer; H.P.W.J.-High Pressure Water Jet; S.Anchor-Skrew Anchor; Bent R.-Bent Rebars; N.R.-No Roughness; W.B.-Wire Brush; R.by Rep.-Rough Surface by Replacement.

Note: Sh.F.-N.C.- Shear Failure in Natural Concrete; T.C.Csh.-Top Concrete Crushed; BT.F.U&T.C.Csh-Brittle Failure at UHPC overlay and Top Concrete Crushed; Sh.Cck-NC&DM-Shear Crack in Normal Concrete and Delamination; Sh.F.-IF-Shear Failure at Interface; Sh.F.p.-IF&p.-NC- Shear Failure partial in Interface and partial in Natural Strength; Cck.-Crack; Csh.-Crush Concrete; D.Sh.-Decrease Shrinkage; D.Cck.-Decrease Crack; Eh.Cck.-Exhibit Crack; F-T.S.-Failed to Provide Adequate Tensile Strength; F.B.-Failure in Bond; W.B.-weak bond; U.L.P.Stress-Undesirable Local Peak Stress; F.Exy.O.- Failure at Epoxy Overlay; P.F.C.S.-Punching Full Cross Section; F.I.-Failure Interface; F.S.-Failure Substrate; F.O.-Failure Overlay; S.F.-Substrate Failure; E.Sh.-Excessive Shrinkage; H.S.P.-High Structural Performance.

Note: C.C.-Conventional Concrete; LMC-Latex Modified Concrete; MMC- Microsilica modified concrete ; MSC- Microsilica Concrete; S.B.Deck-Steel Bridge Deck; LSDC- low slump dense concrete; C.C.+P.F-Conventional Concrete with Polyolefin fiber; A.C.P-Asphalt Concrete Pavement; LWS- Light Weight Sand; CFC-Conventional Fluid Concrete; Old B.D.-Old Bridge Deck; B.Lth.-Bridge Length; dp-depth; dm-diameter; w-width; -: Data not Available; LS- Left Side; T-Top; B-Bottom.

2 EVALUATION OF DATABASE

This section will discuss in detail the factors that have a great influence on the failure of bridge or slab overlay with UHPC and the relation between the substrate and overlay material compressive strength. The most possible failure to occur is a substrate failure as presented in figure 1 combined with table 1. Overall tests were performed on bridges or slabs with compressive strength ranging from 20 to 50 MPa because the basic principle was for strengthening the existing old structures. It is interesting to note that the higher overlay material's compressive strength and a suitable surface preparation let failure mode go through the substrate (Brühwiler & Shen, 2017; F. Xu, Zhou, Chen, Ruan, & Materials, 2014).

In (Ben Graybeal & Haber, 2018) evaluated two types of material for substrate, UHPC, and NSC. Also, with two types of material for overlay UHPC and LMC. The result detected that the failure mode of bridge deck slabs overlay is greatly affected by the types of material designed to be used for overlay, the material constituents, and their strength has a direct effect on the types of failure(Benjamin Graybeal et al., 2020; Huang & Tang, 2010). Figure 1 presented that interface failure happened with the following materials for overlay; low slump dense concrete, epoxy, latex modified concrete fy 3.8 MPa, reinforced concrete fc' for 36 and 37 MPa. In the study (Savino et al., 2020), NSC with 59 MPa compressive strength overlaid with two types of material, the first one was HPFRC fc' 78 MPa, and the second one was UHPC fc' for 147 MPa with high roughness surface preparation for both of them. the result observed that interface failure occurred with HPFRC overlay and substrate failure occurred with UHPC overlay as presented in figure 1. Study (Teng et al., 2021) evaluated three types of materials for overlay, CC, LMC, and UHPC, in result presented that thin layer of UHPC provides better structural performance compared with CC and LMC because the region of failure was at substrate for UHPC and the interface for CC and LMC.

In studies (Ben Graybeal & Haber, 2018; Mohsen A. Issa et al., 2007) failure occurred at overlay. In (Mohsen A. Issa et al., 2007), precast concrete overlaid with LMC 47 MPa compressive strength and MSC 51 MPa compressive strength, both layers bonded by epoxy. Also, in (Ben Graybeal & Haber, 2018) failure occurred at overlay because UHPC fy 5.7 MPa was used for substrate then overlaid with LMC fy 3.8 MPa, and a proper surface preparation was provided for this study by hydro demolition and scarification. As a result, overlay failure occurred because substrate material tensile strength and interface bond strength were higher than overlay material compressive strength.

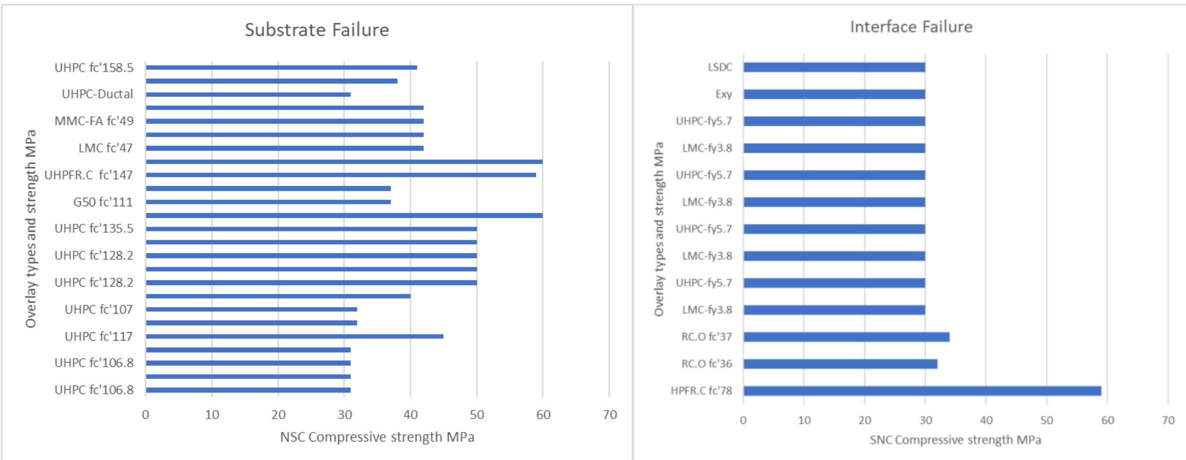

Fig. (1): the effect of Substrate and Overlay material compressive strength on the slab capacity.

2.1 Surface preparation

Different types of substrate surface preparation are suggested in table 1, before strengthening the existing structures. It is important to decide about substrate surface preparation according to the previous experimental studies. In general interface preparation is divided into five basic types including of light preparation, grooved patterns, rough, mechanical connector, and chemical material. Each type subdivided into its group because there are different methods available to reach the desired bond strength. As presented in chart 1, the first one is lightly ground to evaluate

siver.mce20@epu.edu.iq

the ability of overlay material for bond strength without significant roughness. The second type is different patterns of groove surface which different tools and machines are used for this purpose like a wire brush. The third one is the most dependable type and is suggested by many investigators as clarified in chart 1, but the most effective one has exposed rebar which is obtained by eliminating the top layer of substrate concrete until the substrate rebar is exposed. Some other studies like (Lapi et al., 2018) recommended the use of steel tools because sometimes debonding will happen in composite structures which produce a group under the name of the mechanical connector. The last type is the group of chemical materials suggested by several studies to use different types of material to achieve a desirable bond. In another hand, the use of cement grout [C.G.] with a proper surface preparation provides unique bond strength (Lapi et al., 2018). (Brühwiler & Shen, 2017; Mohsen A. Issa et al., 2007) presented that a sufficient bond can be obtained with the Sand Blast technique without causing any damage. A study (Perez et al., 2009) experimented with many techniques to obtain a rough surface, in the result observed that the highest bond strength was obtained with a water-jet and the lowest bond was obtained with a jackhammer. A study (Perez et al., 2009) issued a comparison between two types of surface preparation scarification which are a kind of horizontal groove and hydro demolition is a kind of rough, in the result detected that a better bond was obtained with hydro demolition. (López-Carreño et al., 2020) experimented with the influence of mechanical connectors and concluded that screw anchor can provide adequate bond strength but better structural performance obtained with bent rebar, after two years of traffic 10 % of the slab were cracked but none of them failed at the interface. The study (Muñoz & Ángel, 2012) doesn't recommend using a grooved interface because in all experiments failure occurred at substrate except grooved surface only failure occurred at the interface. (Yang Zhang, Zhang, et al., 2020) highly recommended to use a rough surface because the rough surface can improve interface shear capacity significantly. Also compared with the rough surfaces the smooth, drilled hole, groove, and post-installed rebar interface failure load decreased by 35.2%, 25.9%, 9.4%, and 6.5%. In the study (Yang Zhang, Zhu, et al., 2020) pure shear failure happened at the interface with drilled hole surface preparation. study (Mohsen A. Issa et al., 2007) insisted that the surface preparation hasn't a significant influence alone, the roughness parameters also have to be take into consideration to obtain monolithic structural behavior. Many studies discussed interface texture depth, (Sadek et al., 2019) presented that an adequate bond is obtained with 2 mm texture depth but a better bond can be obtained with deeper texture depth.

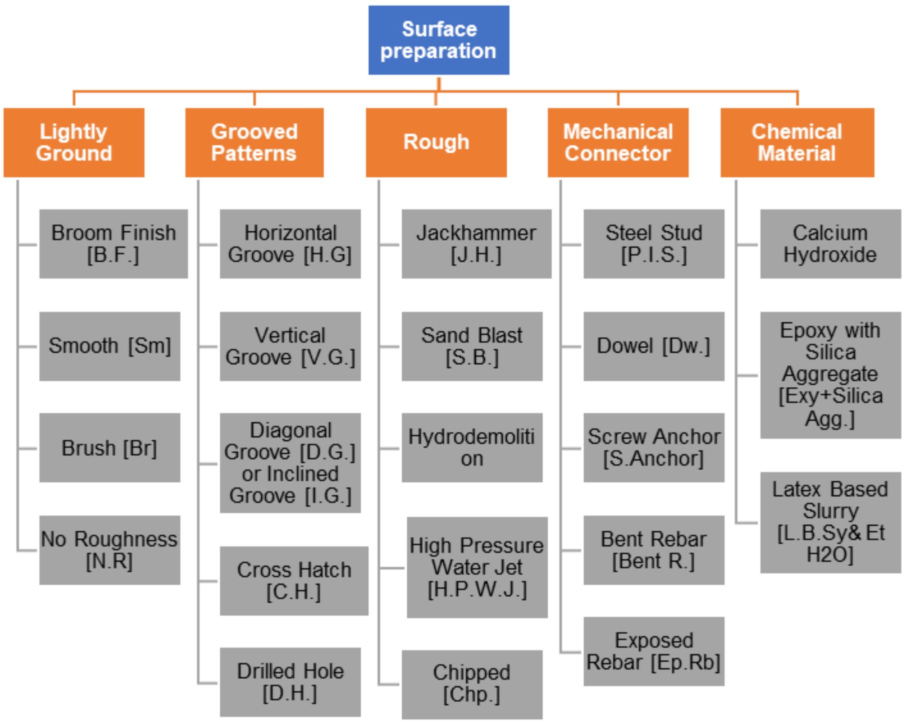

Fig. (2): Types of surface preparation.

Figure 2 presented surface preparation versus ultimate load, there were exist three types of failure; substrate, interface and overlay but it's observed that overlay failure isn't presented in figure 2 because all of them overlaid with UHPC which rarely crack penetrate through it due to its unique matrix. Also, it is important to notice that this figure isn't according to the basic types of surface preparation because each type has different behavior in changing the mode of failure. It is observed that in cases of (rough and inclined groove) surface preparation better bond strength is provided because a failure occurred at the substrate. Figure 2 gives the high value of ultimate load which is due to the smaller cross-section, shorter shear span, or reinforcement ratio compared with the low value because there exist many other parameters that ultimate load depends on. A study (Al-Madani et al., 2022; Yang Zhang, Zhu, et al., 2020; Yang Zhang et al., 2019) observed that better bond strength was obtained with rougher surfaces. The ultimate load increased by 30 % with high roughness at 4.56 mm texture depth and exposed rebars at 4.14 mm roughness depth plus post-installed stud, compared with the grooved joint.

Interface failure is a type of failure that occurs at the contact line between two types of concrete which results in debonding. Common interface failure occurs with smooth surfaces with no roughness, drilled hole, wire brush, grooved joint, and screw anchor as presented in figure 2. Also, it is crucial to understand that this type of failure doesn't occur at the contact line alone, rather than exhibit cracks at NSC and try to separate both concrete layers because failure can't penetrate through the UHPC layer. In (Yang Zhang, Zhang, et al., 2020) observed that with a drilled hole and grooved joint shear failure happened through ultra-high performance tendon and grooved joint, then partially propagated through NSC. In addition, rough surface plus P.I.S. have better bond strength (Yang Zhang et al., 2019) compared with P.I.S alone (Yang Zhang, Zhang, et al., 2020). Also, observed shear failure partially occurred at the interface and partially at NSC with rough 2 mm surface preparation which is rarely a failure that will happen at the interface with rough surface preparation because in most studies of table 1 substrate failure accumulated with rough surface preparation. In (Buitelaar et al., 2004), reported that for steel bridge deck overlay with HPC, three types of surface preparation tri were ed which consists of epoxy with silica aggregate, epoxy with hyper it aggregate, and weld mesh reinforcement but as result due to weak bond interfacial failure happened for all of them. Experimental results showed that the rough surface provides the best structural performance, which is why rough surface preparation is suggested to be used in the future.

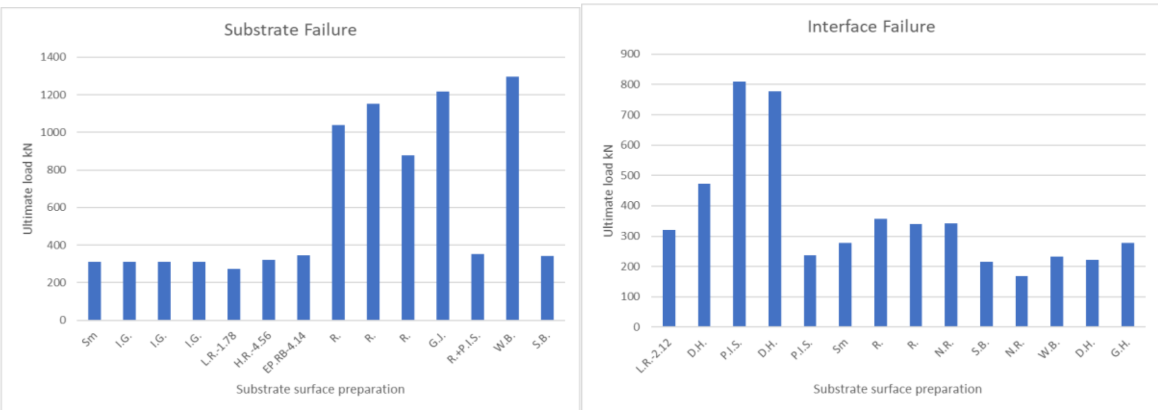

Fig. (3): the effect of substrate NSC surface preparation on the capacity of the composite structure.

2.2 Substrate NSC characterizations

2.2.1 Size effect of substrate material

In (Sritharan & Aaleti, 2017), the slab cross-section size was 609 mm × 203 mm, and the shear span length was 915 mm. Also, the UHPC thickness was 30 mm. In (Wibowo & Sritharan, 2018), the shear span and overlay thickness were the same but the cross-section size was different 2400 mm × 203 mm. comparing studies (Sritharan & Aaleti, 2017; Wibowo & Sritharan, 2018), the effect of varying cross-section size on ultimate load and the ultimate moment was found. In (Sritharan & Aaleti, 2017), all specimens failed with the initiation of shear failure in normal concrete at 311.3 kN ultimate load and 71.17 (kN.m)/m ultimate moment. Also, in the study (Wibowo & Sritharan, 2018) which has a larger cross-section, the ultimate load decreased by 12 % compared with the study (Sritharan & Aaleti, 2017). But it should be

siver.mce20@epu.edu.iq

noted that the slabs have different bond connections.

In (Newtson & Weldon, 2018), studied slab dimensions 900 mm × 900 mm with two different thicknesses, the first one was 101 mm thickness with a 1.1% reinforcement ratio, and the second one was 152 mm thickness with a 0.66% reinforcement ratio. Both slabs are overlaid with 25 mm thickness UHPC without reinforcement and with the same rough surface preparation for the substrate. The result observed that the second slab was exposed to greater shrinkage compared with the first slab and delamination occurred at a higher load than expected. Also, (Gaur & Pal, 2019; Shann, 2012; Q. Xu, Sun, Wang, & Shen, 2009) presented an analytical study about deck slab overlay which determined that debonding and interface shear stress decrease with increased deck thickness, but the deck has a limit for increasing its thickness. This speech isn't compatible with 250 mm or thicker because it increases the distance to the neutral axis which is a reason for tensile cracking stress greater than material strength.

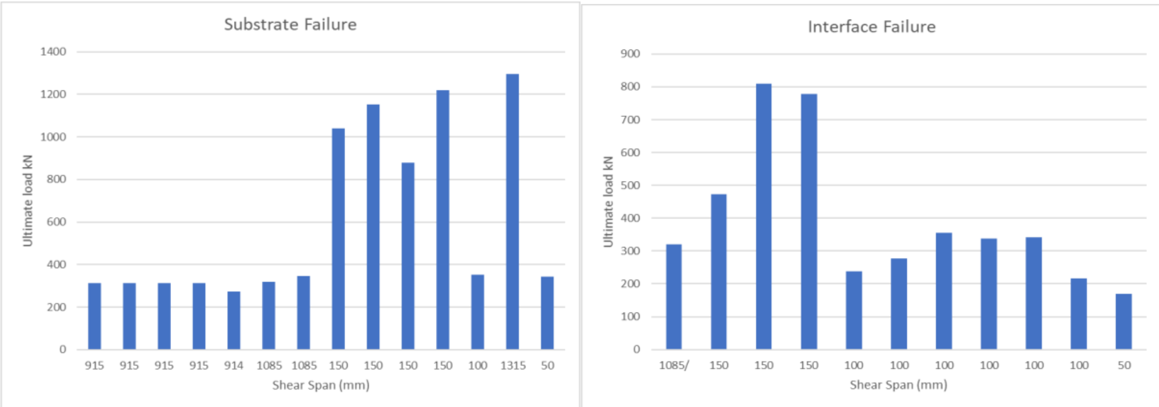

Fig. (4): the effect of shear span on the capacity of the composite structure.

2.2.2 Substrate NSC Compressive strength

Figure 5 combined table 1, presented the effect of substrate natural strength concrete versus ultimate load. Table 1 presented that different substrate materials' compressive strength was experimented with for the strengthening process. However, this parameter has a significant effect on failure mode but it isn't working alone. The effect of NSC compressive strength is comparable with overlay material compressive strength and interface preparation. (Aaleti, Sritharan, & Abu-Hawash, 2013; Ahmed & Aziz, 2015) presented that the failure load of composite structures increases directly with increased NSC compressive strength due to adhesion and cohesion properties between two types of material. (Yang Zhang, Zhang, et al., 2020) evaluated (30,40 and 50) MPa of NSC compressive strength, in result observed that substrate failure happened with 50 MPa compressive strength, while partial interface failure and partial substrate failure happened with 30 MPa and 40 MPa. Until now, limited data related to the effect of the substrate material compressive strength of the strengthened bridge or slab is reported.

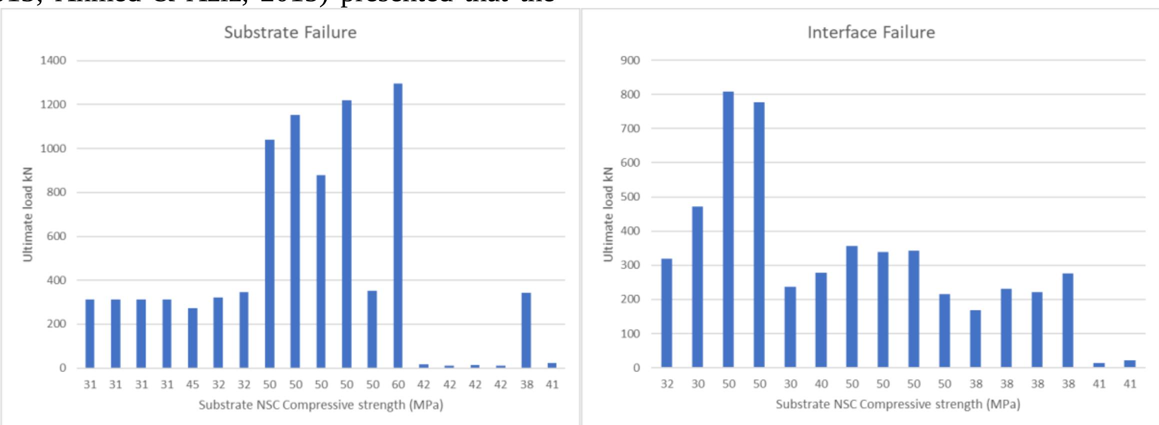

Fig. (5): the effect of substrate NSC compressive strength on the capacity of the composite structure.

2.2.3 Reinforcement ratio in the substrate material

As presented in figure 5 and explained in (Lapi et al., 2018), the existing reinforcement ratio in substrate material changes the mode of failure and increases the ultimate strength. Almost all specimens have a reinforcement ratio in the range from 0% to 1%. In the study (Lapi et al., 2018) reinforcement ratio is 1.8% which is higher than other studies, therefore the debonding between two layers of concrete was observed. It is important to observe that in figure 5 high value of ultimate load resulted from short shear span and the low value resulted from a long shear span. The reinforcement ratio is calculated by equation 1.

$$\rho = \frac{A_{st}}{bh} \quad \dots\dots\dots\dots\dots\dots\dots\dots\dots\dots\dots\dots (1)$$

Where:

A_{st}: longitudinal steel reinforcement

b: cross-section width of unstrengthening slab or bridge

h: cross-section depth of unstrengthening slab or bridge

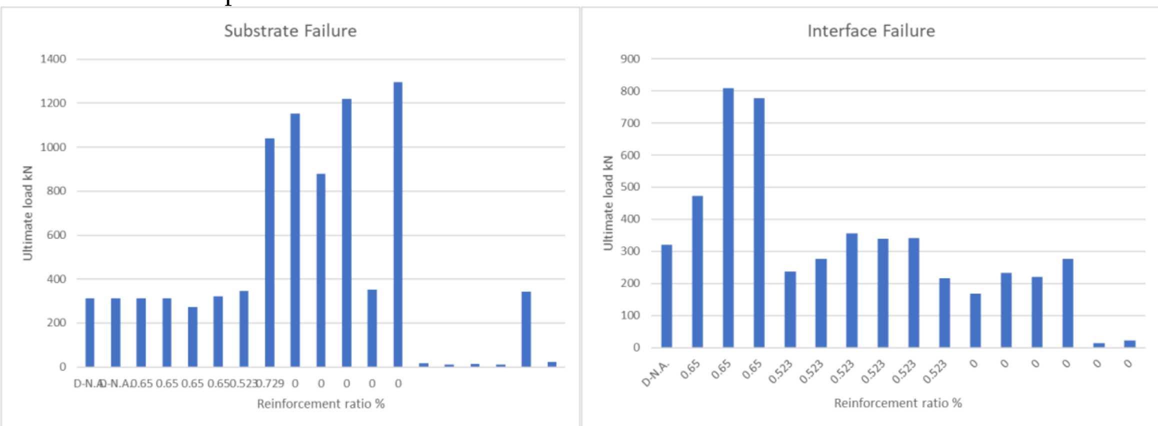

Fig. (6): the effect of substrate reinforcement ratio on the capacity of the composite structure.

2.3 UHPC Overlay characterizations

2.3.1 UHPC thickness

This discussion is related to the increase in ultimate strength versus UHPC thickness as presented in figure 7 which is combined with table 1. UHPC thickness is a crucial parameter that requires significant discussion before the final decision. The high thickness of UHPC on one hand is desirable because tension stress reduces with increased overlay thickness, while on the other hand is undesirable because debonding increases with increased overlay thickness (Shann, 2012; P. Zhang et al., 2021). In the existing experimental studies in table 1, the thickness of the UHPC layer varied from 25 mm to 50 mm. the numerical analysis (Youyou Zhang & Chai, 2021) discussed that 76 mm of UHPC overlay thickness increases the dead load and compressive stress. Also, 20 mm thickness provides tensile stress. But (38-50) mm provide an ideal wearing surface which increases the life of the existing structure and reduces maintenance cost. Based on the existing experimental studies in table 1, the most preferred thickness for the UHPC layer is 50 mm. In (Denmark) 50 mm of UHPC is recommended for use because reduced stress from 124 MPa to 28 MPa. also, (Buitelaar et al., 2004) obtained that (10-12) cm stress reduction factor exists with a 50 mm overlay. Similarly (Teng et al., 2021) issued a study that compared UHPC with CC and LMC, in the result presented that increased UHPC thickness from 25 mm to 50 mm enhance cracking resistance greater than CC and LMC. Therefore, the optimal UHPC thickness is 50 mm depending on the table 1 studies.

siver.mce20@epu.edu.iq

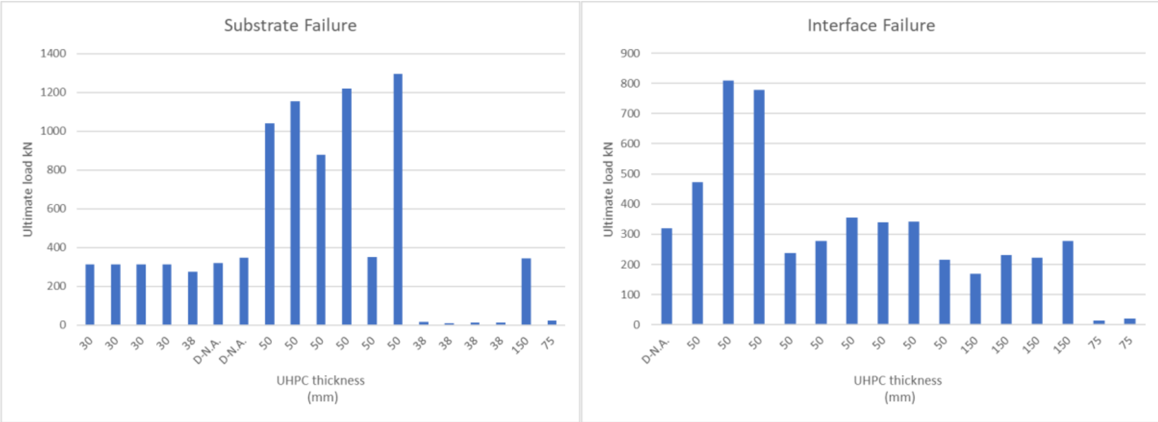

Fig. (8): the effect of UHPC thickness on the capacity of the composite structure.

2.3.2 UHPC Compressive strength

This section is related to the increase in ultimate load versus overlay compressive strength parameter, especially UHPC overlay. This parameter significantly affects the strengthening process. Although different researchers developed different mix proportions and characteristics for overlay the overall aims were similar. The basic principle was to develop the concrete mix that has the unique bond strength for protecting the existing structures. Figure 7 combined with table 1 shows the compressive strength varies with ultimate failure load, the compressive strength ranging from 106 MPa to 170 MPa. In (Mohsen A. Issa et al., 2007; Teng et al., 2021) pull-off test was employed to evaluate the overlay-substrate bond strength, in the result concluded that bond strength directly increases with increased overlay material compressive strength. In addition (Teng et al., 2021) presented that in the composite members overlay crushing occurred with a low material compressive strength, while the increase in bond and ultimate strength was observed in (Bao et al., 2017) with high overlay material compressive strength. (Teng et al., 2021) discussed in detail the use of CC fc' for 37 MPa, LMC fc' 46 MPa, and UHPC fc' for 134 MPa for overlay, in result observed that interface failure happened with CC and LMC overlay but for UHPC overlay failure occurred at substrate because existing steel fiber in overlay material enhances the bond strength (Aziz & Ahmed, 2012; Sharma, Jang, & Bansal, 2022). However, the UHPC compressive strength is a dependable parameter that changes the mode of failure but it is crucial to notice that isn't the only parameter, that is why the ultimate load varied in figure 7.

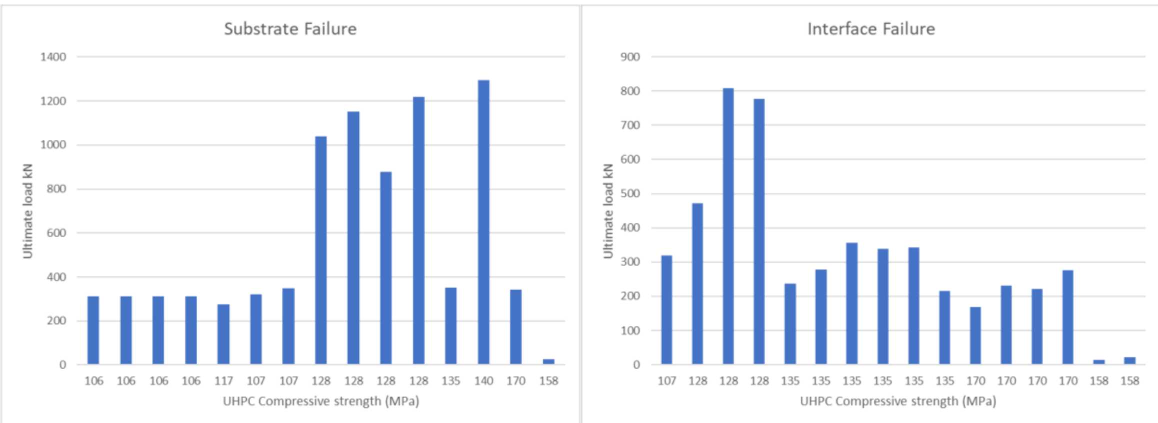

Fig. (7): the effect of UHPC compressive strength on the capacity of the composite structure.

2.3.3 Reinforcement ratio in UHPC

The following discussion is related to the increase in ultimate strength versus steel reinforcement ratio inside the UHPC layer; this parameter is essential and can directly influence the strengthening characterization. This parameter can provide the ability of protection and resistance for the strengthening composite structure. The reinforcement ratio in the overlay layer is calculated by using equation 1. Reinforcement must be embedded in its position to stabilize its structural performance (Wibowo

& Sritharan, 2018). As summarized in table 1 the reinforcement ratio in UHPC overlay ranges from 0% to 4%, which is higher than the reinforcement ratio in substrate concrete, it is because the cross-section area of overlay is lower than unstrengthening substrate material. Figure 9 can observe that with an increased reinforcement ratio in the UHPC layer the ultimate load increases directly. However, this speech isn’t true for all cases because there are many other parameters that can change the mode of failure as mentioned before. In (Brühwiler & Denarié, 2018; Buitelaar et al., 2004; Zhu, Zhang, Hussein, & Chen, 2020) discussed that the steel reinforcement in UHPC overlay can improve structural resistance and durability. Also, it has a significant influence on increasing the load-carrying capacity. Additionally, recommended the use of a 10 mm bar diameter for R-UHPC. However, it is crucial to evaluate the effect of 4 mm or above bar diameters on failure mode but limited data is reported on this topic.

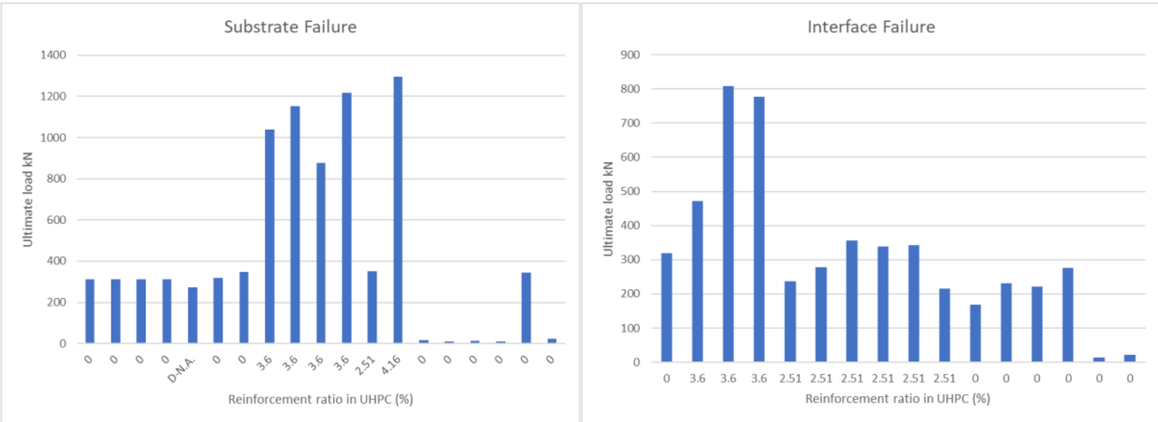

Fig. (9): the effect of UHPC reinforcement ratio on the capacity of the composite structure.

3 PREDICTION EQUATION

Depending on the failure mode of studies in table 1 the prediction equation is proposed to calculate the ultimate load of composite structure NSC-UHPC under flexure. For this purpose, the interpolation polynomial method is used for a set of data to pass through them fitly, and represent the experimental data. In order to create an equation that gives a minimum amount of error the “IBM SPSS Statistics 26” program is used with dependent and independent variables. This equation is summarized in kinds of literature (Hussein et al., 2016; López-Carreño et al., 2020; Luo, 2002; Newtson & Weldon, 2018; Sadek et al., 2019; Sritharan & Aaleti, 2017; Tayeh et al., 2012; Wibowo & Sritharan, 2018; Yang Zhang, Zhang, et al., 2020; Yang Zhang, Zhu, et al., 2020) on studies which have been performed. Equation 2 assists to understand better the flexural performance and predicting the ultimate failure load of the existing NSC structure which is planned to be strengthened with a UHPC overlay.

$$UL = -2162.707 + (0.054\ \mathrm{L}) + (0.372\ \mathrm{W}) + (4.791\ \mathrm{Sth}) + (13.526\ \mathrm{Sfc'}) + (8.316 \times 10^{-12}\ \mathrm{SRr}) + (6.422\ \mathrm{Ofc}) - (144.048\ \mathrm{ORr}) + (7.874\ \mathrm{SP}) \quad \ldots\ldots\ldots\ldots\ldots\ldots (2)$$

Where:

- UL: Ultimate Load (KN)
- L: Length (mm)
- W: Width (mm)
- Sth: Substrate thickness (mm)
- Sfc’: Substrate NSC Compressive strength (MPa)
- SRr: Substrate Reinforcement Ratio %
- Ofc’: Overlay UHPC compressive strength (MPa)
- ORr: Overlay Reinforcement Ratio %

- SP: Surface Preparation

3.1 The basic types of surface preparation are numbered below:

- D.H.-1 D.H.
- G.H.-2 H.G.
- G.J.-3 G.J.
- I.G.-4 I.G.
- N.R.-5 N.R.
- P.I.S.-6 P.I.S.
- R.-7 R.
- R.+P.I.S.-8 R.+P.I.S.
- S.B.-9 S.B.
- Sm-10 Sm
- W.B.-11 W.B.

4 CONCLUSION

- Most specimens strengthened with UHPC at the compression face. However, all studies presented unique properties of UHPC for overlay application but the bond strength is also investigated extensively because the contact line between two types of concrete is viewed as a region of failure. All studies insisted that ultimate strength increase with an increase in the degree of roughness. The rough surface provided the highest bond strength among others, which let composite structures behave monolithically and failure load goes through the substrate.
- For reinforced NSC bridge or slab strengthened with UHPC overlay, showed more affected by substrate parameters. However, a limited number of studies have been available that discussed the influence of substrate thickness on ultimate strength. But still, some studies exist that present that increasing substrate thickness with a limited value induces lower interface shear stress. Substrate material compressive strength can change the mode of failure significantly. The ultimate strength increases with increased substrate material compressive strength due to adhesion/cohesion properties at the interface. A limited number of studies are available that discuss the substrate reinforcement ratio, but the existing studies insisted that increasing the substrate reinforcement ratio with a limited value can reduce shrinkage.
- The experimental results evidenced that ultimate strength was greatly affected by the UHPC characterizations. Overall studies presented that the optimum thickness for UHPC overlay is between 38 mm to 50 mm. However, the ultimate strength increases with increased overlay material compressive strength but a limited number of studies have been available that discuss the effect of this increment on ultimate strength and failure mode. Most studies compared the effect of UHPC strength with other types of concrete. Moreover, the addition of embedded rebar at the UHPC layer tends to conclude shear stress at the interface and normal stress at the UHPC overlay. For bridge deck slabs overlaid with UHPC the mode of failure governed through the substrate while the adequate bond strength is provided by good surface preparation, otherwise interface failure takes place at the contact line or sometimes combined partially at the substrate and partially at the interface. Overall studies noticed that overlay failure never happened with UHPC overlay.

REFERENCES

Aaleti, S., Sritharan, S., & Abu-Hawash, A. (2013). Innovative UHPC-Normal Concrete Composite Bridge Deck. *RILEM-fib-AFGC Int. Symposium on Ultra-High Performance Fibre-Reinforced Concret*, 217-224.

AASHTO. (2017). AASHTO Bridge Design Specification, 8th Ed. In. Washington, DC: American Association of State Highway Transportation Officials.

Ahmed, G. H., & Aziz, O. Q. (2015). *Punching Shear Strength and Behavior of UHPC Flat Plate Slabs* Paper presented at the Thirteenth International Conference on Recent Advances in Concrete Technology and Sustainability, Ottawa, Canada.

Aïtcin, P. C. (2016). Ultra high strength concrete. In *Science and Technology of Concrete Admixtures* (pp. 503-523).

Al-Madani, M. K., Al-Osta, M. A., Ahmad, S., Khalid, H. R., Al-Huri, M. J. C., & Materials, B. (2022). Interfacial bond behavior between ultra high performance concrete and normal concrete substrates. *320*, 126229.

Aldred, J. M., Holland, T. C., Morgan, D. R., Roy, D. M., Bury, M. A., Hooton, R. D., . . . Jaber, T. M. J. A. A. C. I. C. F. H., MI, USA. (2006). Guide for the use of silica fume in concrete. *234*.

Aziz, O. Q., & Ahmed, G. H. (2012). *Mechanical properties of ultra high performance concrete (UHPC).* Paper presented at the Proceedings of the 12th International Conference on Recent Advances in Concrete Technology and Sustainability Issues, Prague, Czech Republic.

Bajaber, M. A., & Hakeem, I. Y. (2021). UHPC evolution, development, and utilization in construction: a review. *Journal of Materials*

Research and Technology, 10, 1058-1074. doi:10.1016/j.jmrt.2020.12.051

Bao, Y., Valipour, M., Meng, W., Khayat, K. H., & Chen, G. (2017). Distributed fiber optic sensor-enhanced detection and prediction of shrinkage-induced delamination of ultra-high-performance concrete overlay. *Smart Materials and Structures, 26*(8). doi:10.1088/1361-665X/aa71f4

Brühwiler, E., & Denarié, E. (2018). Rehabilitation and Strengthening of Concrete Structures Using Ultra-High Performance Fibre Reinforced Concrete. *Structural Engineering International, 23*(4), 450-457. doi:10.2749/101686613x13627347100437

Brühwiler, E., & Shen, X. (2017). *Strengthening of existing structures using R-UHPFRC: principles and conceptual design.* Paper presented at the The 2nd ACF Symposium 2017–Innovations for Sustainable Concrete Infrastructures.

Buitelaar, P., Braam, R., & Kaptijn, N. (2004). *Reinforced high performance concrete overlay system for rehabilitation and strengthening of orthotropic steel bridge decks.* Paper presented at the Orthotropic Bridge Conference, Sacramento, USA.

Denmark, P. B. C. A. Ultra Thin Heavy Reinforced High Performance Concrete Overlays.

Du, J., Meng, W., Khayat, K. H., Bao, Y., Guo, P., Lyu, Z., . . . Wang, H. (2021). New development of ultra-high-performance concrete (UHPC). *Composites Part B: Engineering, 224*. doi:10.1016/j.compositesb.2021.109220

Freeseman, K., Wang, K., & Tan, Y. (2020). Bond strength and chloride resistance of epoxy and concrete overlays on bridge decks. *International Journal of Pavement Engineering*, 1-6. doi:10.1080/10298436.2020.1778693

Gaur, A., & Pal, A. J. I. R. J. O. E. A. (2019). Parametric Study Of Rc Deck Slab Bridge With Varying thickness: A Conceptual Review. *6*, 4978-4983.

Graybeal, B., Brühwiler, E., Kim, B.-S., Toutlemonde, F., Voo, Y. L., & Zaghi, A. J. J. o. B. E. (2020). International perspective on UHPC in bridge engineering. *25*(11), 04020094.

Graybeal, B., & Haber, Z. (2018). Ultra-High Performance Concrete for Bridge Deck Overlays. *U.S.Department of transportation FHWA, 40*, 4-16.

Gunavathy, J., & Indumathi, G. J. B. M. E. (2011). Leadership and Organization Citizenship Behavior-A Study among Employees of a Civil Engineering Company. *4*(1).

Habel, K. (2004). *Structural behaviour of elements combining ultra-high performance fibre reinforced concretes (UHPFRC) and reinforced concrete.* EPFL,

Haber, Z. B., Munoz, J. F., & Graybeal, B. A. (2017). *Field testing of an ultra-high performance concrete overlay*. Retrieved from

Huang, J., & Tang, L. Q. (2010). Mechanism of Early Cracking and Serviceability of Precast Reinforced Concrete Bridge Deck Slabs. *Applied Mechanics and Materials, 34-35*, 1369-1373. doi:10.4028/www.scientific.net/AMM.34-35.1369

Hussein, H. H., Walsh, K. K., Sargand, S. M., & Steinberg, E. P. (2016). Interfacial Properties of Ultrahigh-Performance Concrete and High-Strength Concrete Bridge Connections. *Journal of Materials in Civil Engineering, 28*(5). doi:10.1061/(asce)mt.1943-5533.0001456

Lapi, M., Fernandes, H., Orlando, M., Ramos, A., & Lúcio, V. J. M. o. C. R. (2018). Performance assessment of flat slabs strengthened with a bonded reinforced-concrete overlay. *70*(9), 433-451.

Larsen, I. L., & Thorstensen, R. T. (2020). The influence of steel fibres on compressive and tensile strength of ultra high performance concrete: A review. *Construction and Building Materials, 256*. doi:10.1016/j.conbuildmat.2020.119459

López-Carreño, R.-D., Carrascón, S., Aguado, A., & Pujadas, P. (2020). Mechanical Connectors to Enhance the Interfacial Debonding of Concrete Overlays. *Applied Sciences, 10*(11). doi:10.3390/app10113876

Luo, S. (2002). *Evaluations of concrete overlays for bridge deck applications.* (Master of Science in Civil Engineering), West Virginia University,

Mohsen A. Issa, P. E., M.ASCE, Alhassan, M. A., & Shabila, H. I. (2007). Low-Cycle Fatigue Testing of High-Performance Concrete Bonded Overlay–Bridge Deck Slab Systems. *JOURNAL OF BRIDGE ENGINEERING © ASCE*, 419-428. doi:10.1061/共ASCE兲1084-0702共2007兲12:4共419兲

Muñoz, C., & Ángel, M. (2012). *Compatibility of ultra high performance concrete as repair material : bond characterization with concrete under different loading scenarios.*

Newtson, C., & Weldon, B. (2018). Bridge Deck Overlays Using Ultra-High Performance Concrete. 8&63.

Perez, F., Bissonnette, B., Gagné, R. J. M., & structures. (2009). Parameters affecting the debonding risk of bonded overlays used on reinforced concrete slab subjected to flexural loading. *42*(5), 645-662.

Sadek, H., Toledo, W., Davila, L., Al-Basha, A., Newtson, C., & Weldon, B. (2019). Shrinkage in Ultra-High Performance Concrete Overlays on Concrete Bridge Decks. *MATEC Web of Conferences, 271*. doi:10.1051/matecconf/201927107008

Savino, V., Lanzoni, L., Tarantino, A. M., & Viviani, M. (2020). A cohesive FE model for simulating the cracking/debonding pattern of composite NSC-HPFRC/UHPFRC members. *Construction and Building Materials, 258*. doi:10.1016/j.conbuildmat.2020.119516

Shann, S. V. (2012). *Application of ultra high performance concrete (UHPC) as a thin-bonded overlay for concrete bridge decks.* Michigan Technological University,

Sharma, R., Jang, J. G., & Bansal, P. P. (2022). A comprehensive review on effects of mineral admixtures and fibers on engineering properties of ultra-high-performance concrete,. *Journal of Building Engineering, 45*. doi:https://doi.org/10.1016/j.jobe.2021.103314.

Sritharan, S., & Aaleti, S. (2017). Investigation of A Suitable Shear Friction Interface Between UHPC and Normal Strength Concrete for Bridge Deck Applications. *Bridge Engineering Center and Institute for Transportation Iowa State University, 10*(379), 10-65.

Sritharan, S., Doiron, G., Bierwagen, D., Keierleber, B., & Abu-Hawash, A. (2018). First Application of UHPC Bridge Deck Overlay in North America. *Transportation Research Record: Journal of the Transportation Research Board, 2672*(26), 40-47. doi:10.1177/0361198118755665

Tayeh, B. A., Abu Bakar, B. H., & Megat Johari, M. A. (2012). Characterization of the interfacial bond between old concrete substrate and ultra high performance fiber concrete repair composite. *Materials and Structures, 46*(5), 743-753. doi:10.1617/s11527-012-9931-1

Teng, L., Valipour, M., & Khayat, K. H. (2021). Design and performance of low shrinkage UHPC for thin bonded bridge deck overlay. *Cement and Concrete Composites, 118*. doi:10.1016/j.cemconcomp.2021.103953

Wibowo, H., & Sritharan, S. (2018). Use of Ultra-High-Performance Concrete for Bridge Deck Overlays. *Bridge Engineering Center and Institute for Transportation Iowa State University, 683*, 1-48.

Wu, C., Li, J., & Su, Y. D. (2018). *Development of ultra-high performance concrete against blasts: from materials to structures*: Woodhead Publishing.

Xu, F., Zhou, M., Chen, J., Ruan, S. J. C., & Materials, B. (2014). Mechanical performance evaluation of polyester fiber and SBR latex compound-modified cement concrete road overlay material. *63*, 142-149.

Xu, Q., Sun, Z., Wang, H., & Shen, A. J. J. o. B. E. (2009). Laboratory testing material property and FE modeling structural response of PAM-modified concrete overlay on bridges. *14*(1), 26-35.

Zhang, P., Hu, R., Zou, X., Liu, Y., Li, Q., Wu, G., & Sheikh, S. A. J. C. S. (2021). Experimental study of a novel continuous FRP-UHPC hybrid beam. *261*, 113329.

Zhang, Y., & Chai, Y. (2021). *Numerical analysis of bridge deck rehabilitation by ultra-high-performance concrete (UHPC) overlay.* Paper presented at the Structures.

Zhang, Y., Zhang, C., Zhu, Y., Cao, J., & Shao, X. (2020). An experimental study: various influence factors affecting interfacial shear performance of UHPC-NSC. *Construction and Building Materials, 236*. doi:10.1016/j.conbuildmat.2019.117480

Zhang, Y., Zhu, P., Wang, X., & Wu, J. (2020). Shear properties of the interface between ultra-high performance concrete and normal strength concrete. *Construction and Building Materials, 248*. doi:10.1016/j.conbuildmat.2020.118455

Zhang, Y., Zhu, Y., Yeseta, M., Meng, D., Shao, X., Dang, Q., & Chen, G. (2019). Flexural behaviors and capacity prediction on damaged reinforcement concrete (RC) bridge deck strengthened by ultra-high performance concrete (UHPC) layer. *Construction and Building Materials, 215*, 347-359. doi:10.1016/j.conbuildmat.2019.04.229

Zhu, Y., Zhang, Y., Hussein, H. H., & Chen, G. (2020). Flexural strengthening of reinforced concrete beams or slabs using ultra-high performance concrete (UHPC): A state of the art review. *Engineering Structures, 205*. doi:10.1016/j.engstruct.2019.110035

Zhu, Y., Zhang, Y., Hussein, H. H., Liu, J., & Chen, G. (2020). Experimental study and theoretical prediction on shrinkage-induced restrained stresses in UHPC-RC composites under normal curing and steam curing. *Cement and Concrete Composites, 110*. doi:10.1016/j.cemconcomp.2020.103602

Zhu, Y., Zhang, Y., Hussein, H. H., Qiu, M., Meng, D., Chen, G. J. S., & Engineering, I. (2022). Flexural strengthening of large-scale damaged reinforced concrete bridge slab using UHPC layer with different interface techniques. *18*(6), 879-892.